Virology 535 (2019) 283–296

Contents lists available at ScienceDirect

Virology

journal homepage: www.elsevier.com/locate/virology

Dual role of the amphipathic helix of hepatitis C virus NS5A in the viral polyprotein cleavage and replicase assembly

Yang Zhang[a,1], Xiaomin Zhao[a,1], Jingyi Zou[a], Zhenghong Yuan[a,*], Zhigang Yi[a,b,**]

[a] Key Laboratory of Medical Molecular Virology (MOE/NHC/CAMS), School of Basic Medicine, Shanghai Medical College, Fudan University, Shanghai, China
[b] Department of Pathogen Diagnosis and Biosafety, Shanghai Public Health Clinical Center, Fudan University, Shanghai, China

ARTICLE INFO

Keywords:
HCV
NS5A
Amphipathic helix
Replicase assembly
Polyprotein cleavage

ABSTRACT

Assembling a viral replicase on host intracellular membranes is a common strategy for viral replication of almost all of the positive-strand RNA viruses. Understanding how the key modules of the replicase are involved in the replicase assembly may provide insights into the pathway of the replicase assembly. Herein, by using HCV as a model, we dissect the roles of the amphipathic helix (AH) of NS5A, a key repilcase component, in the viral replicase assembly. The results show that the AH is dispensable for membrane anchoring of NS5A. Instead, AH plays a dual role in the viral replicase assembly: positions a replicase module properly for efficient polyprotein processing and participates in protein-protein interactions within the replicase. This property of AH may serve as an attractive direct anti-viral target.

1. Introduction

Hepatitis C virus (HCV) is a *Flaviviridae* family member. Its infection can cause persistent infection and result in hepatocellular carcinoma (HCC) in the chronically infected individuals. HCV infects approximately 71 million people worldwide (Manns et al., 2017). The HCV genome is a 9.6-kb positive-sense RNA that encodes a single polyprotein. The polyprotein is co- and post-translationally cleaved into at least 10 individual proteins as the order: 5′-C-E1-E2-p7-NS2-NS3-NS4A-NS4B-NS5A-NS5B-3' (see review (Moradpour et al., 2007),). The nonstructural viral protein NS3, NS4A, NS4B, NS5A and NS5B compose the viral replicase for viral replication. The N-terminal portion of NS3 contains a protease domain, using NS4A as the cofactor for the protease. The C-terminal portion of NS3 contains a RNA helicase/NTPase domain. The NS4B is a multi-spanning integral membrane protein and its oligomerization is required for replication complexes assembly. The NS5A is a multifunctional viral protein with non-enzymatic activity and involved in viral replication complex assembly as well as in the virion production. The NS5B is an RNA-dependent-RNA polymerase (see review (Gu and Rice, 2013),).

Like most positive-stranded RNA viruses that replicate in membrane-associated replication complexes (den Boon and Ahlquist, 2010), HCV assembles the replicase in the endoplasmic reticulum (ER), inducing protrusion of the ER to form a double membrane vesicle (DMV) (Romero-Brey et al., 2012). Overexpression of the HCV polyprotein encompassing NS3 to NS5B induces the formation of the similar DMV structure as seen in the virally infected cells (Romero-Brey et al., 2012). Expression of NS5A alone, albeit less efficient, also induces DMV (Romero-Brey et al., 2012), suggesting a critical role of NS5A in the replication complex assembly.

NS5A contains an N-terminal amphipathic helix (AH) in the highly structured domain I (DI), followed by intrinsically disordered domain II (DII) and natively unfolded domain III (DIII). The DI is proposed to mediate NS5A dimerization and RNA-binding (Love et al., 2009; Tellinghuisen et al., 2005). Mutation of DII impairs viral genome replication (Dujardin et al., 2015; Ross-Thriepland et al., 2013a). The DIII is required for virion production (Appel et al., 2008; Verdegem et al., 2011).

Amphipathic helices (AHs) are widely distributed in proteome. It is characterized by the segregation of the hydrophobic and polar residues between the two opposite faces of the α-helix. This unique property gives functional diversities of AH, such as membrane deformation, membrane curvature sensing, specific lipid recognition, coating in lipid droplets (see review (Gimenez-Andres et al., 2018),). Viral proteins also employ AHs for diverse functions. The N-terminal amphipathic helix AH1 and AH2 of HCV NS4B play a dual role in viral replication and virion production (Gouttenoire et al., 2010, 2014). An amphipathic helix of brome mosaic virus protein 1a is required for viral replication

* Corresponding author. Shanghai Medical College, Fudan University, Shanghai, 200032, China.
** Corresponding author. 138 YiXueYuan Road, Shanghai, 200032, China.
E-mail addresses: zhyuan@shmu.edu.cn (Z. Yuan), zgyi@fudan.edu.cn (Z. Yi).
[1] Co-first author.

https://doi.org/10.1016/j.virol.2019.07.017
Received 12 June 2019; Received in revised form 21 July 2019; Accepted 22 July 2019
Available online 24 July 2019
0042-6822/

complex assembly (Liu et al., 2009). An amphipathic helix of influenza virus M2 induces membrane remodeling to drive membrane scission (Martyna et al., 2017). The NS5A AH was previously shown to mediate its membrane association (Brass et al., 2002; Elazar et al., 2003; Penin et al., 2004). Given the central role of HCV NS5A in the viral replicase assembly, dissecting the molecular mechanisms of the NS5A AH in the viral replicase assembly may deepen our understanding of the pathways of viral replicase assembly. In this study, by using a viral replicase assembly surrogate system in which the HCV NS3–5B polyprotein is expressed to mimic the assembly of the viral replicase (Romero-Brey et al., 2012), we dissected the roles of the NS5A AH in the membrane anchoring of NS5A, the viral polyprotein cleavage, and the viral replicase assembly. We found that the AH was dispensable for anchoring NS5A to the membrane. Functional disruption of AH specifically regulated NS5A-NS5B polyprotein cleavage and protein-protein interactions within the replicase. These results point novel roles of the AH in the viral replicase assembly.

2. Results

2.1. NS5A AH is critical for viral replication

To dissect the role of NS5A AH in the replicase assembly process, we first functionally disrupted the AH by deletion or point mutation of AH as reported (Elazar et al., 2003; Gosert et al., 2005), and assessed the viral replication using a subgenomic replicon sgJFH1-sGluc that express a secreted *Gaussia* luciferase (sGluc) (Yi et al., 2016). As expected, deletion of the AH (dAH) or point mutation (NH) to disrupt the AH completely abolished viral replication (Fig. 1). We also replaced the AH with the cognate AHs from HCV related GB virus B (GBV-B) and human pegivirus (HPgV). The AHs form GBV-B and HPgV mediate membrane association of their NS5As as HCV NS5A AH does (Brass et al., 2007). As reported, we verified that replacement of HCV NS5A AH with HPgV AH attenuated viral replication whereas replacement with GBV-B AH abolished viral replication (Fig. 1) (Brass et al., 2007; Romero-Brey et al., 2015).

2.2. The NS5A AH is dispensable for anchoring NS5A to membrane

Next we examined the role of NS5A AH in localizing NS5A in the context of NS3–5B in HEK293T cells. We used a construct to express the JFH1 NS3–5B protein with ypet in frame fused to NS5A (Yi et al., 2016). We also included a construct with a protease inactive mutation (S139A) (Fig. 2A). As expected, the NS5A.ypet contains the wild type AH showed cytoplasmic distribution. The unprocessed NS3–5B.5A.ypet with the protease inactive mutation S139A also showed cytoplasmic distribution (Fig. 2A). Strikingly, the NS5A.ypet with the AH deletion (dAH) or mutation (NH) also showed cytoplasmic distribution either in the context of NS3–5B or NS3–5B.NS3.S139A (Fig. 2A), which is inconsistent with a previous finding that NS5A lacking the AH enters into nucleus in the context of NS3–5B (Gosert et al., 2005). The polyproteins with dAH or NH mutations were efficiently processed, evidenced by cleaved NS3 and NS5A products when determined by Western blotting (Fig. 2B). It was noted that dAH or NH mutations resulted in a reduction of NS5A protein level (Fig. 2B) (see below).

To avoid the potential effect of the in-frame fused ypet on NS5A localization, we examined the distribution of NS5A devoid of ypet by immunostaining with antibody against NS5A (9E10). We also further

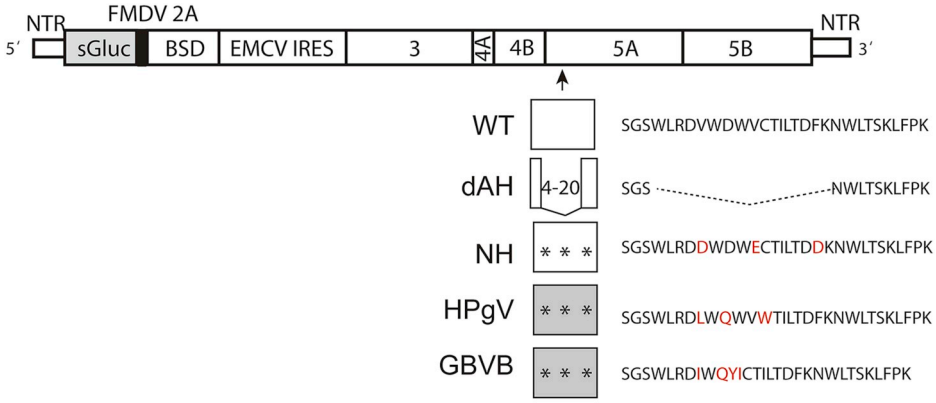

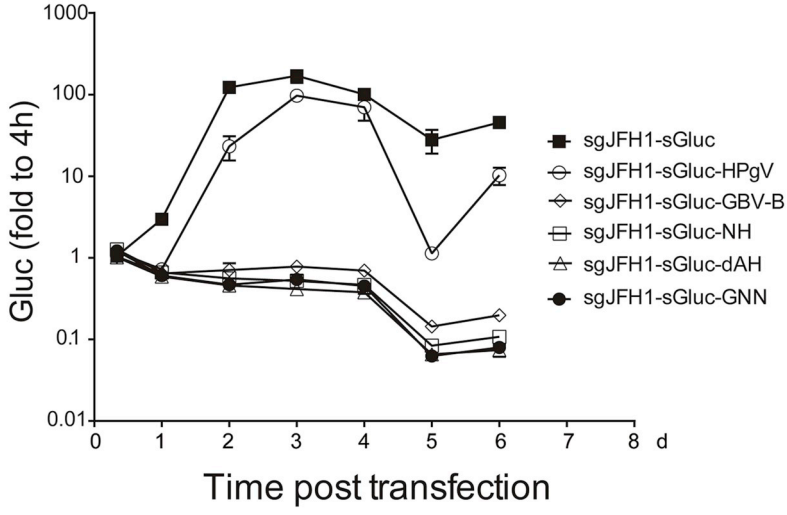

Fig. 1. NS5A AH is critical for viral replication. The upper panel was the schematic of sgJFH1-sGluc and the indicated variants of the NS5A amphipathic helix. The deletion mutations (dashed lines) and point mutations (red) are shown. sGluc, *Gaussia* luciferase; NTR, non-translated region; BSD, balsticidin resistant gene; FMDV 2A (black bar), the foot-and-mouth disease virus 2A autoproteolytic peptide. The bottom panel was the replication of the subgenomic replicons with the above mutations. Replicon RNAs were transfected into Huh7.5 cells in triplicate wells. The supernatants were collected at the time points indicated and the luciferase activity was measured and plotted. The media was refreshed at 4 days post transfection. Mean ± SD are shown (n = 3).

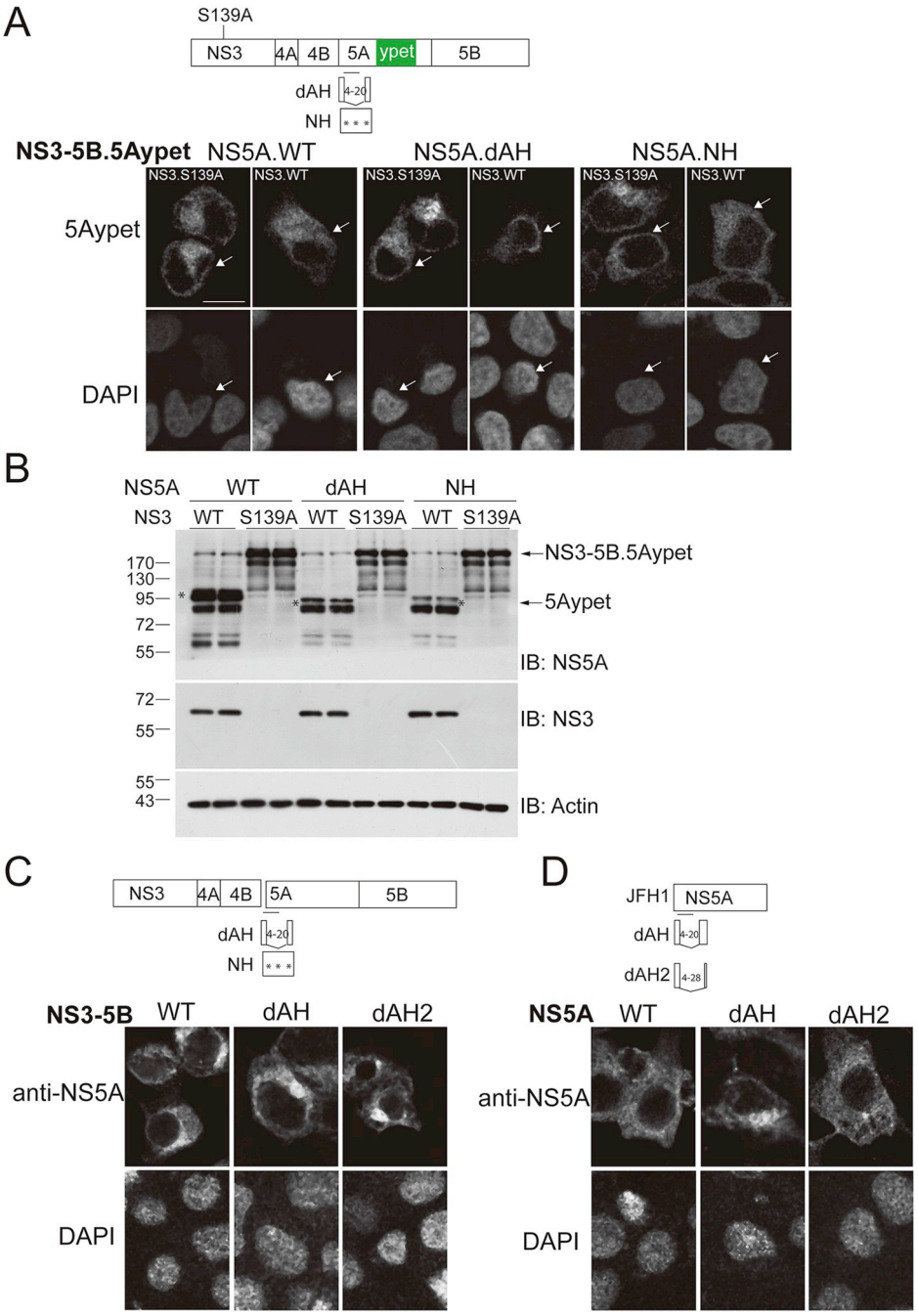

Fig. 2. Distribution of the NS5As bearing AH mutations. (A-B) HEK293T cells were transfected with the plasmids expressing NS3–5B.ypet or the NS5A AH variants. The plasmids contains the wild-type (WT) NS3 or protease inactive NS3 (S139A). The NS3 protease inactive mutation and the NS5A AH mutations (dAH and NH) are shown. (A) Cells were fixed and observed by confocal microscopy. The ypet is in-frame fused in the NS5A. (B) Or the cell lysates were analyzed by Western blotting with antibodies indicated. The asterisks indicate the NS5A variants. (C) HEK293T cells were transfected with the plasmids expressing HCV NS3–5B or the NS5A AH variants (dAH and dAH2). Cells were fixed and immunostained with anti-NS5A antibody and observed by confocal microscopy. (D) HEK293T cells were transfected with the plasmids expressing NS5A or the NS5A AH variants. Cells were fixed, stained with anti-NS5A antibody and observed by confocal microscopy. Representative pictures are shown. Similar results were obtained in three experiments.

truncated the AH to get rid of the entire AH (dAH2) (Fig. 2C, upper panel). The NS5A.dAH and NS5A.dAH2 still showed cytoplasmic distribution in the context of NS3–5B. To exclude the possibility that the cytoplasmic distribution of the NS5A.dAH or dAH2 was due to protein-protein interactions of NS5A with other non-structural proteins in the context of NS3–5B, or due to residual unprocessed NS3–5B, we examined the distribution of NS5A when it was expressed alone. As in the context of NS3–5B, the NS5A.dAH and NS5A.dAH2 also showed cytoplasmic distribution (Fig. 2D). The genotype 1b (BB7) NS5A lacking the AH also showed cytoplasmic distribution (Data not shown). We also examined the localization of the NS5A.dAH and NS5A.dAH2 in Huh7 cells and obtained similar distribution patterns as in the HEK293T cells (Data not shown).

Next, in the context of NS5A.ypet, we examined the distribution of the JFH1 and BB7 NS5A bearing the dAH and NH mutations. We also further deleted the entire domain I (dDI) in the NS5A.dAH mutants to get the dAHdDI mutants. Most JFH1 NS5A.ypet.dAH and NS5A.ypet.NH distributed in the cytoplasm. The JFH1 NS5A.ypet.dAHdDI mainly distributed in the cytoplasm and diffused to the nucleus to some extent (Fig. 3A). Like JFH1 NS5A, the wild type BB7 NS5A.ypet distributed in the cytoplasm whereas the BB7 NS5A.ypet.dAH distributed in the cytoplasm and nucleus. Similarly, the BB7 NS5A.ypet.dAHdDI distributed both in the cytoplasm and in the nucleus (Fig. 3A). To further confirm the membrane association of the NS5A AH mutants in the cytoplasm, we transfected the NS5A mutants into Huh7 cells and fractionated the cells by differential centrifugation into the membrane fraction (P) and the cytosolic fraction (S) either in the presence or absence of 0.5M NaCl (Fig. 3B). We detected the NS5A mutants in each fraction by Western blotting. We detected Calnexin as a membrane protein maker and Hsp70 as a cytosolic protein maker. As expected, Calnexin was exclusively detected in the membrane fractions (P) whereas the majority of the HSP70 were detected in the cytosolic

fraction (S). Like NS5A wild type (WT), nearly 60% of the JFH1 NS5A.dAH were detected in the membrane fraction, either in the presence or absence of 0.5M NaCl (Fig. 3C–D), suggesting a membrane association of NS5A.dAH. In contrast, most of the JFH1 NS5A.dAHdD1 mutants were detected in the cytosolic fraction (S) (Fig. 3C–D). Similarly, the BB7 NS5A.ypet mainly resided in the membrane fraction. Like the wild type, the majority of the BB7 NS5A.ypet.dAH were detected in the membrane fraction, whereas most of the BB7 NS5A.ypet.dAHdDI were detected in the cytosolic fraction (Fig. 3E–F). Thus, the domain I but not the AH is required for the membrane association of JFH1 and BB7 NS5As.

It was reported that deletion of a genotype 1 NS5A AH resulted in

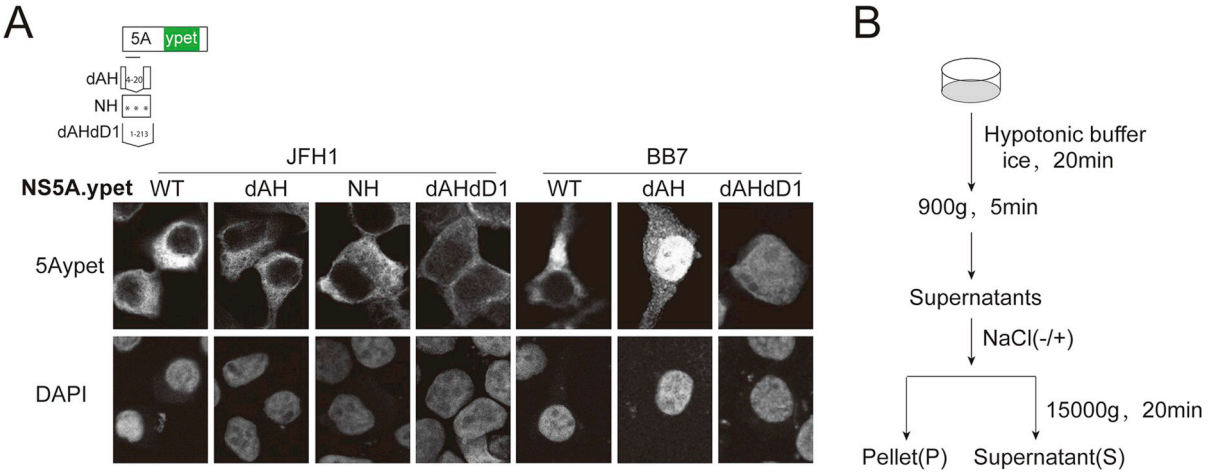

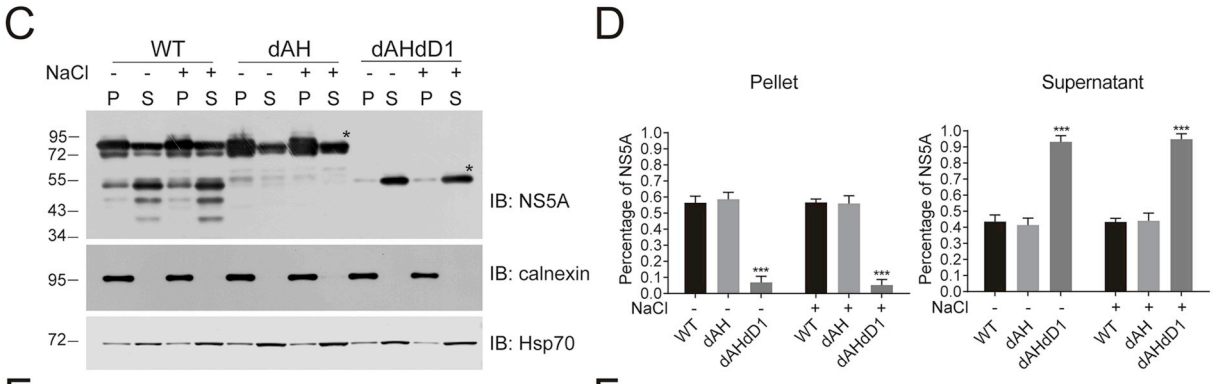

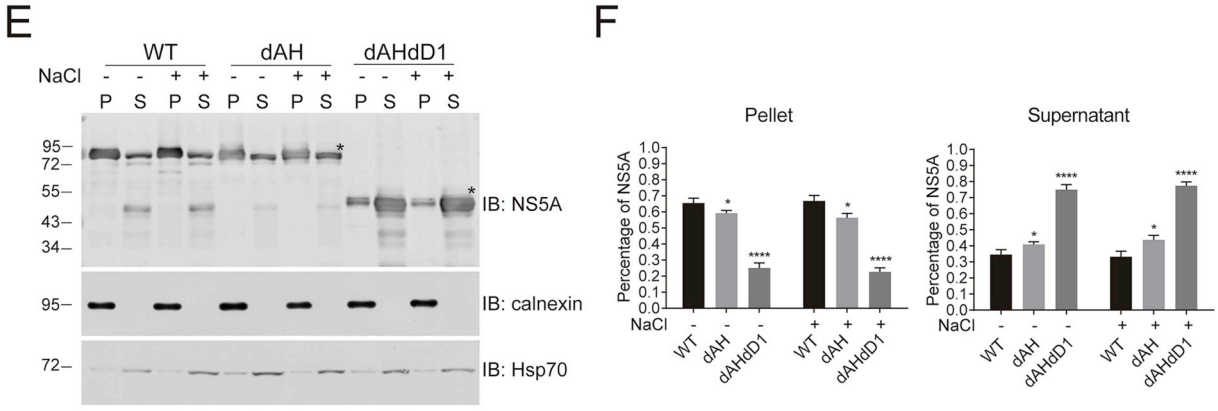

G

Strain	Predicted NLS	Score
H77	PPPRKKRTVVL	9
BB7	PPPRRKRTVVL	4.7
JFH1	PPPRRRRTVGL	5.2
HCV 3a	PPPRRKRTTQL	3.6
HCV 4a	PSPRRKRTVQL	4.2
HCV 5	PLPRRKRKPMEL	12
HCV 6a	PPPRRKRLVRL	3.5

(caption on next page)

Fig. 3. AH was dispensable for anchoring NS5A to the membrane. (A) HEK293T cells were transfected with the plasmids expressing NS5A.ypet or the NS5A variants. Cells were fixed and observed by confocal microscopy. (B) The schematic of the experiment design of cell fractionation. (C) Huh7 cells were transfected with the plasmids expressing NS5A.ypet or the NS5A variants. Cells were disrupted by hypotonic buffer, and the postnuclear lysates were treated with 0.5M NaCl or not, then separated by centrifugation into a crude membrane fraction (pellet, P) and a cytosolic fraction (supernatant, S). Proteins in the fractions were analyzed by Western blotting. (D) The NS5A protein abundances in C were quantified and the proportion of NS5A in the pellets (P) and the supernatants (S) were calculated respectively. Mean ± SD are shown (n = 3). Data combined from three experimental replicates. (E) Huh7 cells were transfected with the plasmids expressing NS5A.ypet (BB7) or the NS5A variants. Cells were separated by into membrane fraction (pellet, P) and a cytosolic fraction (supernatant, S) as in C. Proteins in the fractions were analyzed by Western blotting. (F) The NS5A protein abundances in E were quantified and the proportion of NS5A in the pellets (P) and the supernatants (S) were calculated respectively. Mean ± SD are shown (n = 3). Data combined from three experimental replicates. Statistical analysis was performed between the variants and the WT groups. (*$P < 0.5$; ***$P < 0.001$; ****$P < 0.0001$; two-tailed, unpaired *t*-test). The values to the left of the blots C and E are molecular sizes in kilodaltons. (G) The NS5A sequences of different HCV strains were analyzed by NLS Mapper software (http://nls-mapper.iab.keio.ac.jp/cgi-bin/NLS_Mapper_form.cgi) for NLS prediction. The sequences and scores of the predicted NLS are shown.

nuclear localization of NS5A probably due to the presence of the nuclear localization signal sequence (Gosert et al., 2005). Our results suggest absence of NLS in the JFH1 NS5A whereas presence of NLS in the BB7 NS5A. The H77 NS5A has a strongly predicted NLS (score of 9, by NLS mapper software) whereas JFH-1 (score of 5.2) lacks a strongly predicted NLS (Fig. 3G), which is consistent with our experiment results. Although the BB7 NS5A lacks a strongly predicted NLS (score of 4.7), it contains a highly similar sequence with the NLS of H77 NS5A with only one amino acid difference (Fig. 3G), which may explain the nuclear localization of the BB7 NS5A.ypet.dAHdDI observed in this study (Fig. 3A).

2.3. AH regulates NS5A phosphorylation and protein level

In this study, we did not observe nuclear localization of JFH1 NS5A AH mutants, which is probably due to the absence of nuclear localization signal of JFH1 NS5A. However, the absence of nuclear localization of the AH mutants gives us the opportunity to study the effects of AH mutants on viral replicase assembly.

As we noted that the dAH and NH mutations resulted in the reduction of NS5A.ypet protein level in the context of NS3–5B (Fig. 2B), we then carefully examined the protein levels of the NS5A variants bearing the dAH, NH mutations and the replaced cognate AHs in the context of NS3–5B (Fig. 4A). We expressed the NS3–5B variants in Huh7 cells, and detected viral proteins by Western blotting. All the AH mutations or replacements did not affect the NS3 protein level. In contrast, dAH and NH mutations resulted in both the reduction of basal level and hyper phosphorylation level of NS5A (Fig. 4B) whereas replacement of AH with GBV-B and HPgV AHs did not affect the basal level but reduced the hyper phosphorylation level of NS5A (Fig. 4B).

To examine the effect of AH mutations replacements on the NS4B protein level, we used the NS3–5B.NS4B.HA plasmid to express the NS5A variants with an HA-tagged NS4B (Paul et al., 2013; Zhang et al., 2019). Similarly as in the context of NS3–5B, the dAH and NH mutations dramatically reduced the basal and hyper phosphorylation level of NS5A (Fig. 4B) whereas replacement of AH with GBV-B and HPgV AHs only reduced the hyper phosphorylation level of NS5A. In contrast, the dAH and NH mutations and the AH replacements did not affect the protein levels of NS3 and slightly affected the protein levels of NS4B (Fig. 4C).

2.4. AH regulates the trans-cleavage of NS5A-NS5B

To explore if the reduction of NS5A protein level is due to inefficient polyprotein cleavage, we examined the processing of the polyproteins bearing the AH mutations. Given that the AH mutations did not affect NS3 protein level (Fig. 4B–C), we focused on the processing of the NS4B-5A-5B, 4B-5A and 5A-5B. As the N-terminus of NS4B adopts dual topology (Lundin et al., 2003), to generate authentic N-termini of the viral proteins, we in-frame fused a ubiquitin monomer to the N-termini of the polyproteins (Fig. 5A, upper panel). The ubiquitin fusion protein should be cleaved by cellular ubiquitin carboxy-terminal hydrolase to produce the authentic N-terminal residues of viral proteins (Bachmair

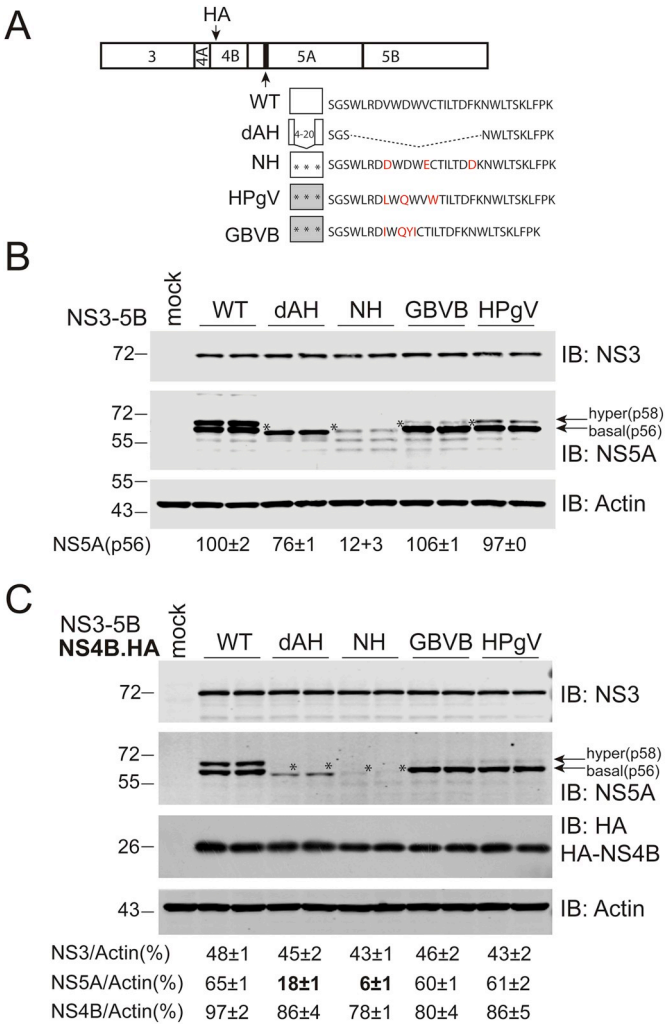

Fig. 4. NS5A AH regulates NS5A phosphorylation and protein level. (A) Schematic of the AH mutants in the context of NS3–5B. The sequences of NS5A AH variants are shown. An HA tag is inserted in between the AH1 and AH2 of NS4B in C. (B) Cells in duplicated wells were transfected with the plasmids expressing HCV NS3–5B or the NS5A AH variants as indicated. Cell lysates were analyzed by Western blotting with antibodies indicated. The asterisks indicate the NS5A variants. The basal level of NS5A (p56) was quantified and the relative levels were shown (Mean ± SD, n = 2). Representative pictures are shown. (C) Huh7 cells were transfected with the plasmids expressing HCV NS3–5B.NS4B.HA or the NS5A AH variants and the cell lysates were analyzed as in B. The protein levels of NS3, NS5A (p56) and NS4B were quantified and normalized to the protein levels of Actin (Mean ± SD, n = 4). Data combined from two independent experiments done in duplicates are shown. The values to the left of the blots B and C are molecular sizes in kilodaltons.

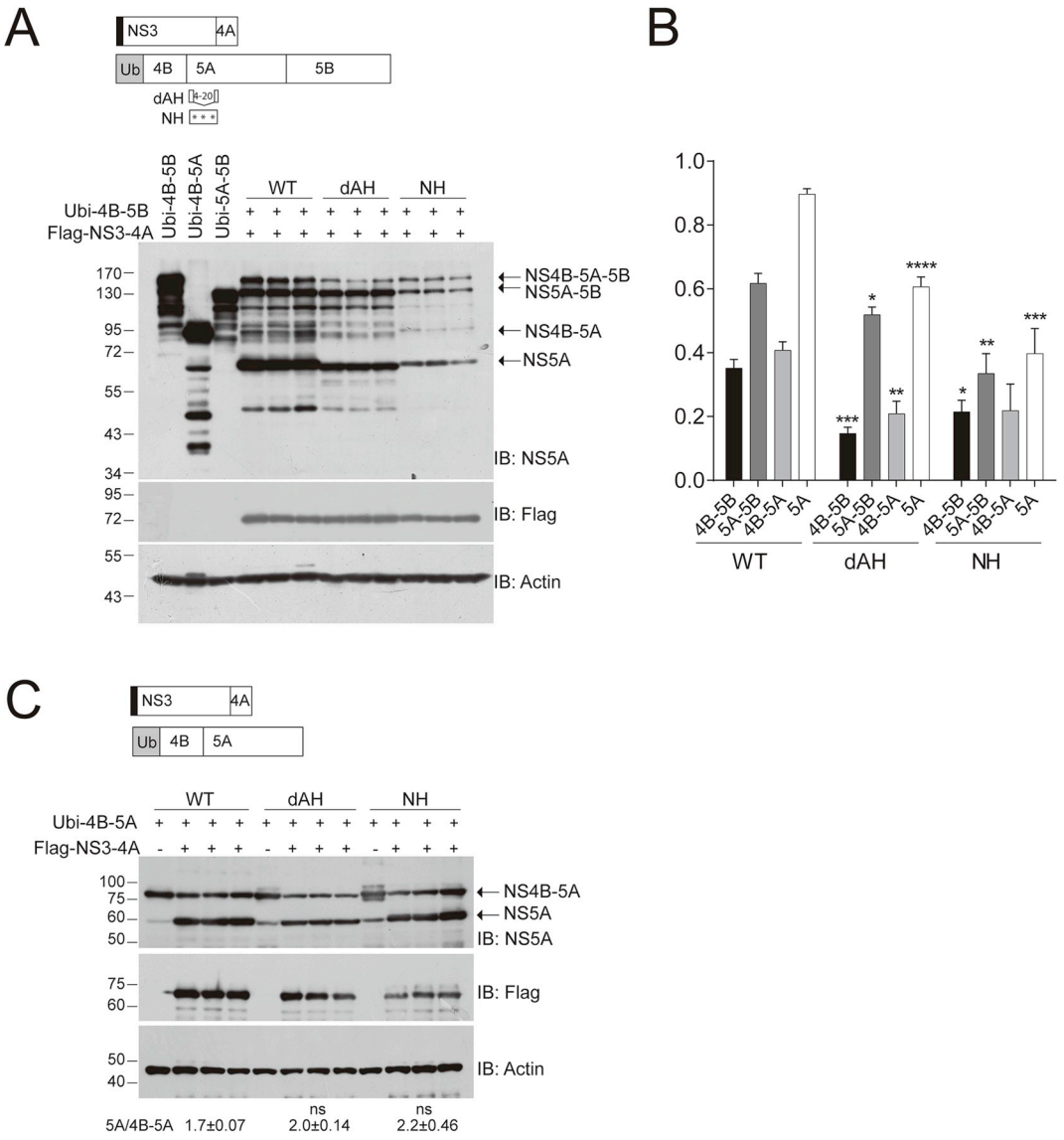

Fig. 5. *Trans* cleavage of NS4B–5B bearing NS5A AH mutations. (A) Schematic of the constructs used is shown in the upper panel. Ub (grey box), ubiquitin. The NS3-4A contains an N-terminal 3 × Flag (Black bar). The NS5A AH mutants are shown. The plasmids expressing the Ubi-NS4B–5B or NS5A AH variants were co-transfected with the plasmid expressing Flag-NS3-4A into HEK293T cells in triplicated wells. The proteins were analyzed by Western blotting with antibodies indicated. Representative picture are shown. (B) The protein (arrows) abundances of A from two independent experiments done in triplicates were quantified and calculated. Mean ± SEM are shown (n = 6). (C) The plasmids expressing the Ubi-NS4B-5A or NS5A AH variants were co-transfected with the plasmid expressing Flag-NS3-4A into HEK293T cells. The proteins were analyzed by Western blotting. The protein (arrows) abundances were quantified and the ratios of the cleaved NS5A to its precursor NS4B-NS5A were calculated. Mean ± SEM are shown (n = 7). Representative data from three independent experiments done in triplicates or duplicates are shown. Statistical analysis was performed between the AH variants and the WT groups. (ns, not significant; $^{*}P < 0.5$; $^{**}P < 0.01$; $^{***}P < 0.001$; $^{****}P < 0.0001$; two-tailed, unpaired *t*-test). The values to the left of the blots A and C are molecular sizes in kilodaltons.

et al., 1986; Lin et al., 1994). We co-transfected the plasmids encoding the polyproteins and the NS3-4A in the HEK293T cells and examined the NS3-4A-mediated *trans*-cleavage of the polyproteins. The high transfection efficiency and high expression levels of the polyproteins in HEK293T cells provided the opportunity to detect the processed intermediates by Western blotting. HEK293T cell supports replication of the JFH1 subgenomic replicon (Kato et al., 2005), making it physiologically relevant to study the polyprotein processing in these cells. Upon co-expression with NS3-4A, the NS4B-5A-5B could be processed *in trans* to produce the NS5A and the intermediates (Fig. 5A, arrows). Comparing with the wild type (WT), dAH and NH mutations retarded the polyprotein processing, evidenced by the reduction of the protein levels of NS5A, NS4B-5A (Fig. 5B). To explore which cleavage site is affected by the mutations, we first focused on the 4B-5A cleavage. When co-expressed in the HEK293T cells, the Ubi-4B-5A was processed *in trans* by the NS3-4A to the produce NS5A. The dAH and NH mutations did not significantly affect the cleavage efficiency of 4B-5A as judged by the ratio of the protein level of NS5A to the precursor NS4B-5A (Fig. 5C).

Then we monitored the cleavage of NS5A-5B. We co-expressed the Ubi-5A-5B and NS3-4A in either HEK293T cells or Huh7 cells and monitored the cleavage efficiency of the NS5A-5B. We found that the dAH and NH mutations significantly reduced the cleavage efficiency of the NS5A-5B (NS5A/NS5A-5B) either in the HEK293T cells (Fig. 6A) or in the Huh7 cells (Fig. 6B). To rule out the possibility that the reduction of the cleavage efficiency of the NS5A-5B is due to the reduction of the NS5A protein stability caused by dAH and NH, we examined the protein expression of the Ubi-NS5A bearing the dAH and NH mutations. In both the HEK293T cells (Fig. 6C) and the Huh7 cells (Fig. 6D), the dAH and NH mutations did not significantly reduced the NS5A protein levels. These data demonstrate that disruption of AH impairs the polyprotein

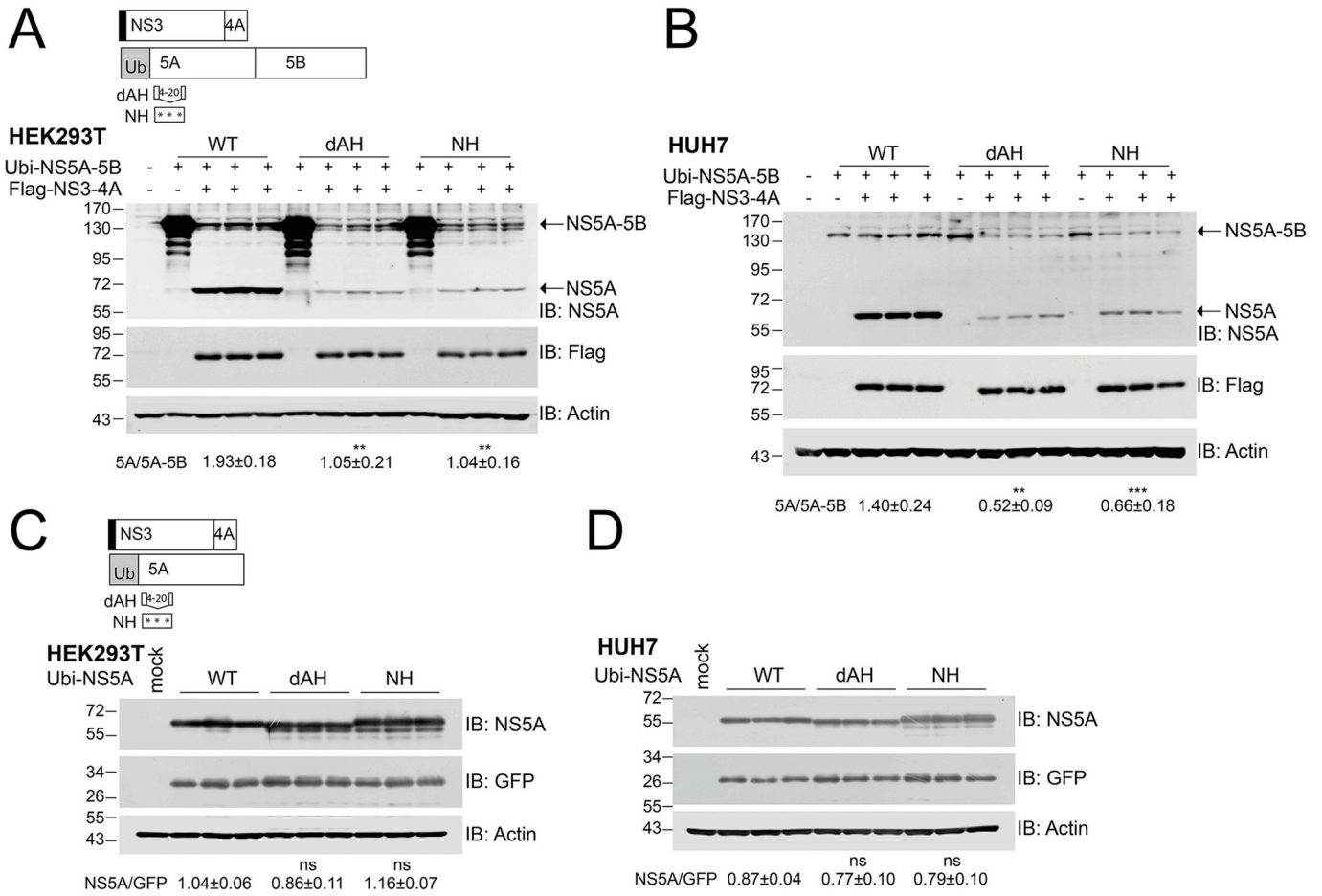

Fig. 6. NS5A AH mutations impair NS5A-NS5B cleavage. The plasmids expressing the Ubi-NS5A-5B or NS5A AH variants were co-transfected with the plasmid expressing Flag-NS3-4A into triplicated HEK293T cells (A) or Huh7 cells (B). The proteins were analyzed by Western blotting with antibodies indicated. Representative pictures are shown. The protein (arrows) abundances were quantified and the ratios of the cleaved NS5A to its precursor NS5A-NS5B were calculated. Mean ± SEM are shown (n = 9). Representative data from three independent experiments done in triplicates are shown. Statistical analysis was performed between the AH variants and the WT groups as indicated. (**$P < 0.01$, ***$P < 0.001$; two-tailed, unpaired *t*-test). The plasmids expressing the Ubi-NS5A or NS5A AH variants were co-transfected with the plasmid expressing GFP into HEK293T cells (C) or Huh7 cells (D). The protein abundances of the NS5A and GFP were quantified and the ratios of the NS5A to GFP were calculated. Mean ± SEM are shown (n = 6). Representative data from two independent experiments done in triplicates are shown. Statistical analysis was performed between the AH variants and the WT groups as indicated. (ns, not significant; two-tailed, unpaired *t*-test). The values to the left of the blots are molecular sizes in kilodaltons.

processing at the NS5A/NS5B site.

2.5. AH regulates protein-protein interactions within the replicase components

Given that the replacement of AH with AHs from GBV-B and HPgV did not affect the polyprotein processing (Fig. 4), but abolished or attenuated viral replication (Fig. 1), we reasoned that in addition to regulating the NS5A-5B processing, AH might also regulate protein-protein interactions within the replicase components. We used a replicase assembly surrogate system that the NS3–5B polyprotein is expressed with the HA-tagged NS5A or HA-tagged NS4B without abolishing the viral replication (Zhang et al., 2019). We expressed the NS3–5B with AH variants in the Huh7 cells and then immunoprecipitated against the HA-NS5A or HA-NS4B and assessed the protein-protein interactions of the HA-tagged proteins with another replicase component NS3. We normalized the protein interactions by calculating the IP efficiency as the ratio of the (immunoprecipitated NS3/ input NS3) to the (captured NS5A or NS4B.HA/input NS5A or NS4B.HA). Comparing with the wild type (WT), all the AH mutations (dAH, NH, GBV-B and HPgV) significantly reduced the NS5A-NS3 interactions (Fig. 7A–B). Similarly, the mutations also significantly reduced the NS4B-NS3 interactions (Fig. 7C–D).

2.6. Disruption of the AH renders NS4B more sensitive to proteinase K digestion in the digitonin-permeabilized cells

The replicase components interact with each other to assemble the replicase. We recently reported that NS5A inhibitor daclatasvir (DCV) allosterically impairs the NS4B-involved protein-protein interactions within the viral replicase and disrupts the replicase quaternary structure (Zhang et al., 2019). Given that the AH regulates the protein-protein interactions within the replicase components, we sought to explore the impact of functional disruption of AH on the quantery structural change of the replicase. We have demonstrated that in the digitonin-permeabized cells, the NS4B's sensitivity to proteinase K (PK) digestion reflects the protection of the full-length NS4B by the proteinacous replicase and the changes of the NS4B's sensitivity to PK may reflect a quaternary structural change of the replicase (Zhang et al., 2019)(see discussion). Here, we took a similar strategy, and expressed the NS3–5B.NS4B.HA bearing the NS5A AH variants and then permeabilized the cells by digitonin and digested the permeabilized cells by PK (Fig. 8A). The proteins' sensitivity to PK digestion was assessed by Western blotting with antibodies against different replicase

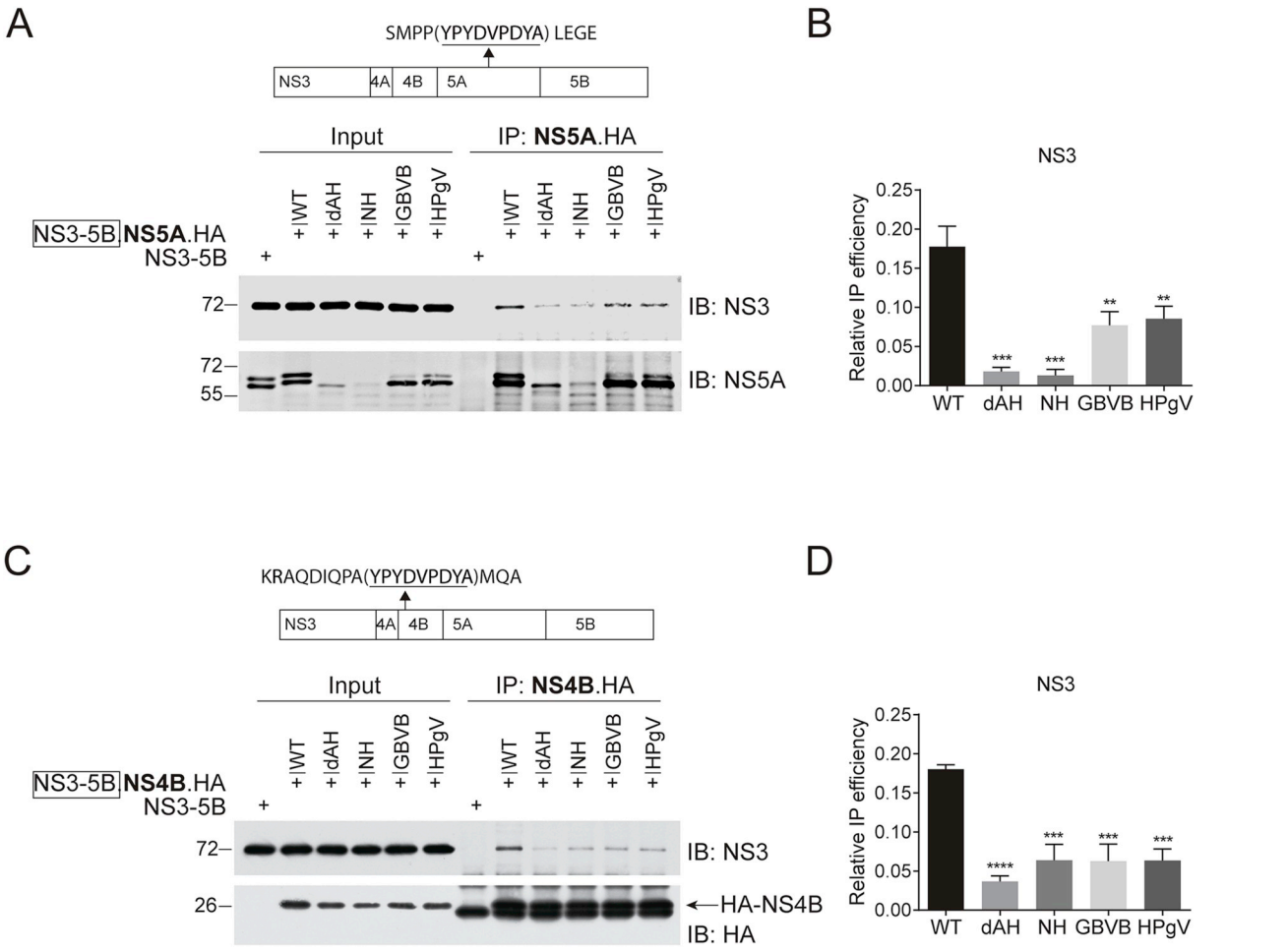

Fig. 7. AH regulates protein-protein interactions within the replicase components. (A) Triplicated Huh7 cells were transfected with the plasmids expressing HCV NS3–5B.NS5A.HA or NS3–5B.NS5A.HA containing the NS5A AH variants. Cells were lysed and the cell lysates were captured by anti-HA beads. The captured proteins were analyzed by Western blotting with the antibodies indicated. The cell lysate from NS3–5B-transfected Huh7 cells was used as a negative control. (B) The relative immunoprecipitation (IP) efficiency in A was calculated as (immunoprecipitated NS3/ input NS3)/ (captured NS5A.HA/input NS5A.HA). Mean values ± SD are shown (n = 3). Data combined from the triplicated wells. Similar results were obtained in another independent experiments. (C) Huh7 cells were transfected with the plasmids expressing HCV NS3–5B.NS4B.HA or NS3–5B.NS4B.HA containing the NS5A AH variants. Cells were lysed and cell lysates were captured by anti-HA beads and analyzed as described in A. The asterisks indicate the NS5A variants. (D) The relative immunoprecipitation (IP) efficiency was calculated as (immunoprecipitated NS3/ input NS3)/ (captured NS4B.HA/input NS4B.HA). Mean values ± SD are shown (n = 3). Data combined from the triplicated wells. Similar results were obtained in another independent experiments. Statistical analysis was performed between the AH variants and the WT groups as indicated. (**$P < 0.01$, ***$P < 0.001$, ****$P < 0.0001$; two-tailed, unpaired t-test).

components (Fig. 8B). The PK digestion efficiency was evidenced by complete digestion of the C-terminal cytoplasmic domain of Calnexin while the N-terminal domain residing in the endoplasmic reticulum (ER) lumen remained intact (Fig. 8C). As the NH mutation dramatically reduced the protein level of the NS5A, making it difficult to judge the NS5A's sensitivity to PK digestion (Fig. 8C). Except for the NH, all the AH mutants did not affect the NS3's and the NS5A's sensitivity to PK digestion (Fig. 8D–E). In contrast, all the mutants increased the NS4B's sensitivity to PK (Fig. 8F). These data indicate that functional disruption of the AH may induce quaternary structural change of the replicase.

2.7. Impact of some replication-null mutations in other region of NS5A and in the region of NS5B on the protein-protein interactions within the replicase components and the quaternary structure of the replicase

To demonstrate the specificity of the AH mutations-induced phenotypes, we introduced some reported mutations that abolish viral replication (replication-null) in the regions of NS5A other than the AH and in the NS5B region (Fig. 9A). The S235A mutation is located in the NS5A LCS I, and the phosphorylation at S235 probably regulates NS5A interaction with host factor human homologue of the 33-kDa vesicle-associated membrane protein-associated protein (hVAP33) (Chong et al., 2016). The C338A mutation is located in the C-terminus of NS5A DII, which is probably participate in the interaction with the host factor cyclophilin A (CypA)(Ross-Thriepland et al., 2013b). The V321E mutation is located in NS5B and within a hydrophobic cavity of the polymerase (Lam et al., 2014). First, we tested the impact of S235A, C338A, and V321E mutations on protein-protein interactions within the replicase components. We introduced these mutations in the NS3–5B expression system as described in Fig. 6, in which NS5A and NS4B are HA-tagged, respectively. Then assessed the HA-NS5A and HA-NS4B interactions with the NS3, respectively. We found that neither the C338A nor the S235A mutation affected the NS5A-NS3 (Fig. 9B–C) and the NS4B-NS3 (Fig. 9D–E) interactions, whilst the V321E mutation in NS5B slightly increased the NS5A-NS3 and the NS4B-NS3 interactions (Fig. 9C–E).

We then examined the viral proteins' sensitivity to PK digestion when the NS3–5B.NS4B.HA plasmids bearing the NS5A variants were expressed. Comparing with the wild type, all the mutations C338A,

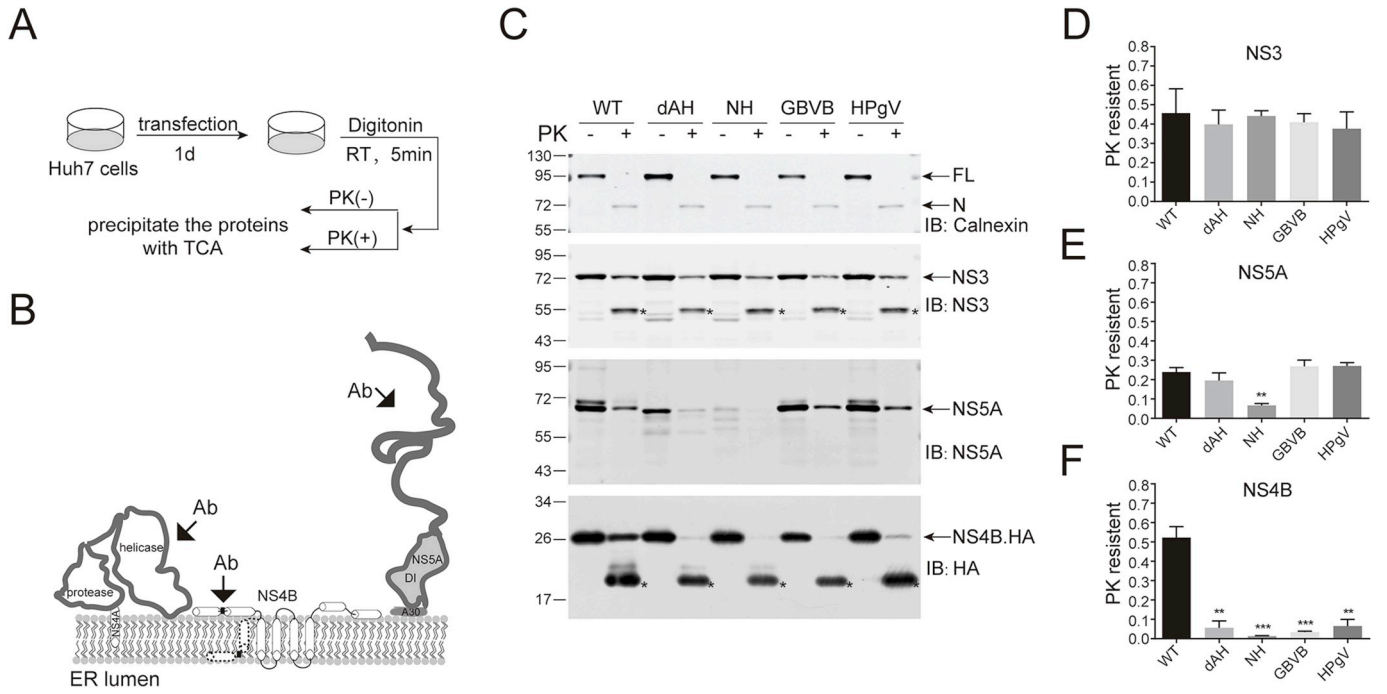

Fig. 8. Abolishing AH disrupts the quantery structure of the replicase. (A) The schematic of the experiment design of proteinase K digestion. (B) The schematic of the topology of the replicase components and the antibody recognition sites of NS3, NS5A and NS4B. (C) The Huh7 cells expressing the NS3–5B.NS4B.HA or NS3–5B.NS4B.HA containing the NS5A AH variants were permeabilized with 50μg/ml digitonin, scraped, and resuspended in buffer C. The permeabilized cells were treated (+) or not (-) with 10 μg/ml proteinase K (PK) for 5min at 37°C and then precipitated by TCA and the proteins were analyzed by Western blotting with the antibodies indicated. FL, full-length calnexin; N, protected N-terminal calnexin. The asterisks indicate proteolytic fragments. Similar results were obtained in multiple independent experiments. (D-F) The protein abundances in C were quantified and the PK-resistant efficiency was calculated as the ratio of the undigested protein (PK +) to the total protein (PK-). Mean values ± SD are shown (n = 3). Data combined from triplicated wells. Statistical analysis was performed between the AH variants and the WT groups as indicated. (**$P < 0.01$; ***$P < 0.001$; two-tailed, unpaired *t*-test.)

S235A, V321E did not affect the NS3, NS4B, and NS5A's sensitivity to PK. In contrast, the dAH mutation significantly reduced NS4B's sensitivity to PK as deserved above (Fig. 9F–I).

3. Discussion

Amphipathic helices (AHs) are widely used by viral proteins for important functions. HCV NS4B is a multi-spanning integral membrane protein. There are structurally resolved amphipathic alpha-helix AH1 and AH2 in its N-terminal part. The AH1 is essential for viral replication complex assembly and involved in virus production (Gouttenoire et al., 2014). AH1 is overall hydrophilic and does not directly interact with membrane (Gouttenoire et al., 2009). The AH2 is required for viral replicase assembly probably through oligomerization (Gouttenoire et al., 2010). AH2 has a very hydrophobic side and can traverse the lipid bilayer to give a dual topology of NS4B. It is proposed that in the dual topology model, AH1 associated with the inner side of the ER membrane induces or senses membrane curvature during membranous web formation (Gouttenoire et al., 2014). AH1 may also participate in intra- or inter-molecular interactions with other viral proteins for virion production (Gouttenoire et al., 2010, 2014).

The HCV NS5A AH was previously shown to mediate its membrane association (Elazar et al., 2003). It is reported that deletion of NS5A AH resulted in nuclear localization of NS5A probably due to the presence of the nuclear localization signal sequence (Gosert et al., 2005). In this study, we found that deletion or functional mutation of AH did not change the cytoplasmic distribution of NS5A in the context of NS3–5B polypeptide or NS5A alone (Figs. 2 and 3) and did not affect the membrane association of JFH1 NS5A and BB7 NS5A (Fig. 3C–F). The discrepancy might be due to the different genotypes of NS5A. The H77 NS5A contains a strongly predicted NLS but the JFH1 NS5A contains a weak predicted NLS (Fig. 3G). Although the BB7 NS5A contains a weak predicted NLS, it was capable to enter into nucleus, suggesting the presence of a functional NLS (Fig. 3A). The nuclear localization of NS5A may mask many phenotypes of AH deletion in the past studies such as membrane association of NS5A. In this study, we found that deletion of NS5A AH did not change the membrane association of JFH1 and BB7 NS5As but further deletion of DI impaired membrane association of the NS5As (Fig. 3), suggesting a critical role of DI in the membrane association of NS5A and a different role of AH in viral replication. NS5A DI mediates dimerization of NS5A *in vitro* and *in vivo* (Love et al., 2009; Shanmugam et al., 2018; Tellinghuisen et al., 2005). The dimerization of DI might generate a hydrophobic surface for membrane association or some loops in the DI might act as the intertwined loop of *flaviviruse* NS1 to mediate the membrane association (Xu et al., 2016).

Deletion or functional mutation of NS5A AH specifically impaired the polyprotein processing at the NS5A/NS5B site (Figs. 5 and 6) and the protein-protein interactions within the replicase components (Fig. 7). Experiment of proteinase K digestion of the digitonin-permeabilized cells shows that deletion or functional mutation of NS5A AH renders NS4B more sensitive to proteinase K digestion (Fig. 8), which is analogue to the phenotype of NS5A inhibitor daclatasvir-treated cells (Zhang et al., 2019). We have demonstrated that the proteinase K sensitivity of NS4B reflects the quaternary structure of the replicase but is not due to the change of the morphology of the virus-induced vesicles, as several replication-null NS4B point mutants that either form multiple membrane vesicle (MMV) or single membrane vesicle (SMV) both increase NS4B's sensitivity to proteinase K (Zhang et al., 2019). The disruption of the replicase might be due to the retarded polyprotein processing at NS5A/NS5B site (Fig. 6), which is in line with a previous finding that proper polyprotein cleavage kinetics is essential for HCV replicase assembly (Romero-Brey et al., 2015).

NS5A AH may also directly participate in protein-protein interactions, as replacement of the NS5A AH with GBV-B and HPgV NS5A AH

that inhibits or attenuates viral replication (Fig. 1) did not affect the polyprotein processing (Fig. 4) but reduced the protein-protein interactions within the replicase components (Fig. 7) and disrupted quaternary structure of replicase (Fig. 8). This is further supported by the finding that the AH mutations reduced hyper-phosphorylation of NS5A (Fig. 4B–C) and hyper-phosphorylation of NS5A may need the protein-protein interactions among the viral proteins (Koch and Bartenschlager, 1999) and regulate viral protein interaction with host factors to assemble the replicase (Evans et al., 2004). There is evidence for genetic interaction between NS5A AH and NS4B (Biswas et al., 2016). If there are physical interactions between NS5A AH with other replicase components needs further studies.

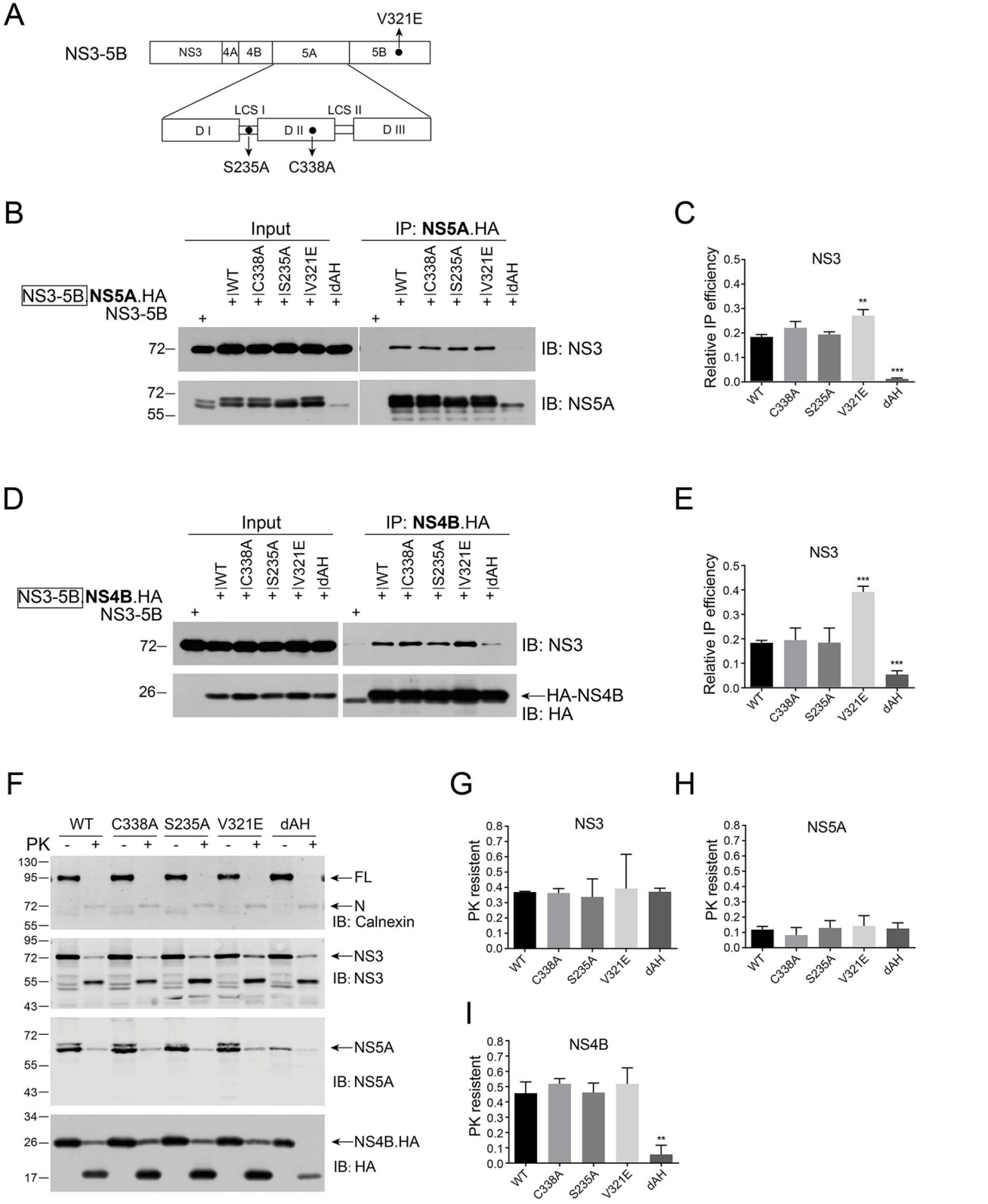

(caption on next page)

Fig. 9. Impact of replication-null mutations in other region of NS5A and in the region of NS5B on the protein-protein interactions within the replicase components and the quaternary structure of the replicase. (A) The schematic of NS5A and NS5B variants. (B) Huh7 cells were transfected with the plasmids expressing the HCV NS3–5B.NS5A.HA or NS3–5B.NS5A.HA contains the indicated mutations. The cell lysates were captured by anti-HA beads and the captured proteins were analyzed by Western blotting. (C) The relative immunoprecipitation (IP) efficiency in B was calculated as above. Representative picture is shown. Mean values ± SEM are shown (n = 6). Data combined from two independent experiments done with triplicated wells (D) Huh7 cells were transfected with the plasmids expressing the NS3–5B.NS4B.HA or NS3–5B.NS4B.HA contains the indicated mutations. The cell lysates were captured by anti-HA beads and the captured proteins were analyzed by Western blotting. (E) The relative immunoprecipitation (IP) efficiency in D was calculated as above. Mean values ± SEM are shown (n = 6). Data combined from two independent experiments done with triplicated wells (F) Huh7 cells expressing the NS3–5B.NS4B.HA or NS3–5B.NS4B.HA containing the indicated mutations were permeabilized and digested by PK as above. Proteins were analyzed by Western blotting with the antibodies indicated. (G-H) The protein abundances in F were quantified and the PK-resistant efficiency was calculated. Mean values ± SD are shown (n = 3). Data combined from triplicated wells. Statistical analysis was performed between the AH variants and the WT groups as indicated. (**$P < 0.01$; ***$P < 0.001$; two-tailed, unpaired *t*-test.)

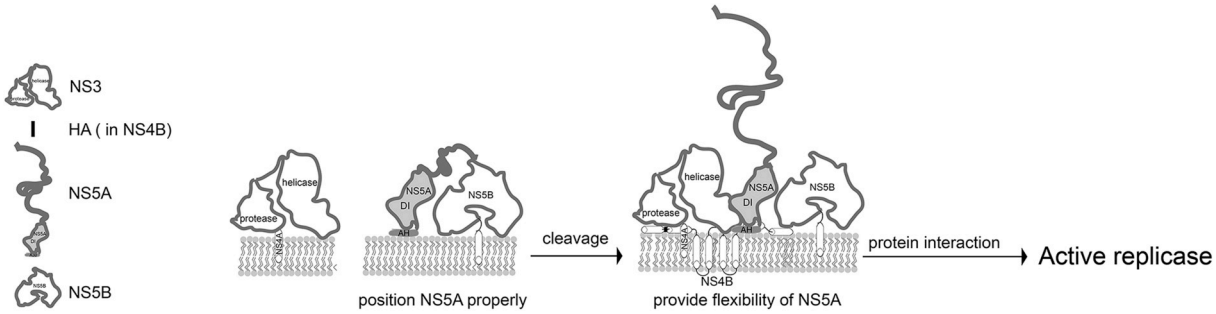

Fig. 10. A proposed model for the role of AH in HCV polyprotein cleavage and replicase assembly. The viral proteins may exist as multimers *in vivo*. Only the monomers are shown. The NS3 consists of the N-terminal protease domain and the C-terminal helicase domain. NS3 associates with the membrane by interacting with NS4A. NS4B is a multi-spanning integral membrane protein. The HA tag (black bar) is inserted in-frame into between the first (AH1) and the second amphipathic helix (AH2). NS5A associates with membrane via the N-terminal amphipathic helix (AH) (Grey). Concerted protein-protein interactions within the replicase components induce assembly of the active replicase on the endoplasmic reticulum (ER), resulting in protruding of the ER membrane. The protruded ER membrane is further modified to form a double membranous vesicle (DMV), namely the replication complex. NS5A AH may play a dual role in the replicase assembly, it positions the NS5A properly to facilitate the *trans*-cleavage at NS5A/NS5B site by NS3-4A; in addition, NS5A AH may provide the flexibility of NS5A movements required for precise protein-protein interactions and participate in the protein-protein interactions within the replicase components.

The AH-mediated polyprotein processing is separable from the AH-mediated protein-protein interaction as the replacement of HCV NS5A AH with cognate NS5A AHs of GB virus B (GBV-B) and human pegivirus (HPgV) did not affect polyprotein processing (Fig. 4B–C). We propose that NS5A AH plays a dual role in the replicase assembly. Rather than mediating membrane association, it positions the NS5A properly to facilitate the *trans*-cleavage at NS5A/NS5B site by NS3-4A and this function is replicable by the cognate AHs of GBV-B and HPgV. In addition, NS5A AH may provide the flexibility of NS5A movements required for precise protein-protein interactions and participate in the protein-protein interactions within the replicase components and this function is partially replicable by the HPgV but not replicable by the GBV-B (Fig. 10). An amphipathic alpha-helix of brome mosaic virus (BMV) protein 1a is required for viral replication complex assembly (Liu et al., 2009). This peripheral membrane protein induces membrane modification and recruits viral polymerase and RNA templates to assemble the viral replicase of BMV. Mutagenesis studies show that the AH of BMV 1a participate in two separable functions, one is membrane association and induction of membrane invagination and the other one is recruitment of viral polymerase. Mutations inhibiting the membrane association increase the polymerase accumulation whilst there are mutations that maintain the membrane association but fail to recruit the polymerase (Liu et al., 2009). The dual role of HCV NS5A AH in the HCV replicase assembly may point a conserved function of AHs in the positive-strand RNA virus.

4. Materials and methods

4.1. Plasmids

To generate the subgenomic replicon sgJFH1-sGluc expressing a secreted *Gaussia* luciferase (sGluc), using the sgJFH1 (Yi et al., 2016) as a backbone, first a cassette containing the sGluc-2A fragment was assembled with a cassette containing the BSD-EMCV IRES by fusing PCR and then the assembled fragments was digested by AgeI/KpnI and ligated into the similarly digested sgJFH1 to get the plasmid sgJFH1-sGluc. The NS5B inactive mutation GNN was introduced by fusion PCR-mediated mutagenesis to get the plasmid sgJFH1-sGluc-GNN. The plasmid sgJFH1-sGluc-dAH with deletion of the 4–20 amino acids of the NS5A AH, plasmid sgJFH1-sGluc-dAH2 with deletion of the 4–28 amino acids of the NS5A AH, plasmid sgJFH1-sGluc-NH with point mutations to disrupt the NS5A AH (Elazar et al., 2003), plasmid sgJFH1-sGluc-GBVB with a replacement of the HCV NS5A AH with GBV-B, and plasmid sgJFH1-sGluc- HPgV with a replacement of the HCV NS5A AH with HPgV (Romero-Brey et al., 2015), were generated by fusion PCR-mediated mutagenesis. Plasmid pFlag-NS3-4A were described previously (Yi et al., 2011) and the NS3 inactive mutation S139A was introduced by fusion PCR-mediated mutagenesis to get the plasmid pFlag-NS3-4A.S139A. Plasmid phCMV-3-5B expressing the NS3-NS5B and phCMV-3-5B.ypet expressing an in-frame fused ypet in the NS5A were reported previously (Yi et al., 2016). To generate the plasmid phCMV-3-5B.5A.HA expressing an HA-tagged NS5A in the context of NS3–5B, an SanDI/BsrGI digested fragment was swapped from the plasmid sgJFH1-NS5A.HA (Yi et al., 2016) into the similarly digested plasmid phCMV-3-5B. A PmlI fragment containing the HA-tagged NS4B was swapped from sgJFH1-NS4B.HA (Yi et al., 2016) into phCMV-3-5B to get the plasmid phCMV-3-5B.NS4B.HA. ClaI/SanDI Fragments containing the NS5A amphipathic helix mutations were swapped from the sgJFH1. dAH, sgJFH1. NH, sgJFH1. GBVB and sgJFH1. HPgV into the phCMV-3-5B to get the plasmids phCMV-3-5B. dAH, phCMV-3-5B·NH, phCMV-3-5B.GBVB and phCMV-3-5B.HPgV, respectively; into the plasmid phCMV-3-5B.5A.HA to get the plasmids phCMV-3-5B.5A.HA.dAH, phCMV-3-5B.5A.HA.NH, phCMV-3-5B.5A.HA.GBVB and phCMV-3-5B.5A.HA.HPgV, respectively. ClaI/SanDI Fragments containing the NS5A amphipathic helix mutations were swapped from the sgJFH1. dAH, sgJFH1. NH, into the plasmid phCMV-3-5B.ypet to get the

plasmids phCMV-3-5B.ypet.dAH and phCMV-3-5B.ypet.NH, respectively. A PmlI fragment containing the HA-tagged NS4B was swapped from sgJFH1. NS4B.HA (Yi et al., 2016) into the plasmids phCMV-3-5B·NH and phCMV-3-5B.HPgV to get the plasmids phCMV-3-5B.4B.HA.NH and phCMV-3-5B. 4B.HA.HPgV, respectively. To generate plasmid phCMV-Ubi-NS4B–5B, first a ubiquitin sequence flanked with a BglII site was assembled with an NS4B-5A fragment containing the SanDI site, and then the assembled fragment was cloned into the BglII/SanDI site in the phCMV-3-5B to replace the original fragment. Similarly, to generate plasmid phCMV-Ubi-NS5A-5B, first a ubiquitin sequence was assembled with NS5A fragment and then the assembled fragment was ligated into the BglII/SanDI site in the phCMV-3-5B. Using phCMV-Ubi-NS4B–5B as template, the Ubi-NS4B-NS5A region was amplified and cloned into BglII/EcorI site in phCMV to plasmid phCMV-Ubi-NS4B-5A. To generate plasmids phCMV-Ubi-NS4B–5B.dAH, phCMV-Ubi-NS4B–5B·NH, phCMV-Ubi-NS4B-5A.dAH and phCMV-Ubi-NS4B-5A.NH, fragments that encompasses the PmlI/SanDI region and contains the NS5A amphipathic helix were amplified by PCR from the dAH and NH containing plasmids described above and then ligated into the PmlI/SanDI sites in phCMV-Ubi-NS4B–5B and phCMV-Ubi-NS4B-5A, respectively. To generate phCMV-Ubi-NS5A-5B.dAH, phCMV-Ubi-NS5A-5B·NH, phCMV-Ubi-NS5A.dAH and phCMV-Ubi-NS5A.NH, NS5A regions bearing the mutations were fused with Ubi by fusion PCR and cloned into phCMV by BglII/EcorI. To generate phCMV-NS5A.ypet.dAH, phCMV-NS5A.ypet.NH, phCMV-NS5A.ypet.dAHdD1, phCMV-NS5A, phCMV-NS5A.dAH, phCMV-NS5A.dAH2 and phCMV-NS5A.NH, the NS5A regions were amplified by PCR from the phCMV-3-5B.ypet.dAH, phCMV-3-5B.ypet.NH, phCMV-3-5B, phCMV-3-5B.dAH and phCMV-3-5B·NH, respectively, and then cloned into the BglII/EcorI sites in phCMV. Plasmid phCMV-3-5B.ypet (BB7) expressing an in-frame fused ypet in the NS5A were reported previously (Yi et al., 2016). To generate phCMV-NS5A.ypet.dAH (BB7) and phCMV-NS5A.ypet.dAHdD1 (BB7), the NS5A regions were amplified by fusion PCR from the phCMV-3-5B.ypet (BB7), and then cloned into the BglII/MfeI sites in phCMV. To generate plasmid phCMV-Ubi-NS5A, phCMV-Ubi-NS5A.dAH, phCMV-Ubi-NS5A.NH, first a ubiquitin sequence was assembled with NS5A fragment and then the assembled fragment was ligated into the BglII/SanDI site in the phCMV-NS5A. To generate phCMV-3-5B.4B.HA.S235A, phCMV-3-5B.4B.HA.C338A, phCMV-3-5B.4B.HA.V321E and the phCMV-3-5B.5A.HA.S235A, phCMV-3-5B.5A.HA.C338A, phCMV-3-5B.5A.HA.V321E, NS5A mutations S235A, C338A and the NS5B mutation V321E were introduced into the plasmid phCMV-NS3-5B.4B.HA and phCMV-NS3-5B.5A.HA by fusing PCR-mediated mutagenesis. All of the constructs were proofed by Sanger DNA sequencing. Detailed information is available upon request.

4.2. Cells

The human embryonic kidney cell line HEK293T, human hepatoma cell line Huh7 (Cell Bank of the Chinese Academy of Sciences, Shanghai, China, www.cellbank.org.cn) and Huh7.5 (kindly provided by Charles Rice) were routinely maintained in Dulbecco's modified medium supplemented with 10% FBS (Gibco) and 25mM HEPES (Gibco) with non-essential amino acids (Gibco).

4.3. In-vitro transcription

XbaI-linearized plasmids were purified and used as templates for the *in-vitro* transcription by MEGAscript T7 Transcription Kit (Ambion) according to the manufacturer's protocol. The RNAs were purified by RNeasy Mini kit (Qiagen).

4.4. Antibodies

Anti-NS5A monoclonal antibody (9E10; gifted by Charles Rice) that recognizes the domain III of NS5A (Romero-Brey et al., 2015) was used in Western blotting and immunofluorescence analyses at 1:2000 and 1:200 dilutions, respectively. Anti-NS3 monoclonal antibody (Virogen; 217-A) that recognizes the helicase domain (a.a. 1350–1460) was used at 1:1000 dilution in Western blotting; Anti-β-actin antibody (Sigma; A1978) was used at 1:4000 dilution in Western blotting; Anti-calnexin antibody (BD; 610523) was used at 1:2000 dilution in Western blotting; Anti-HA antibody (Roche; clone 3F10) was used at 1:000 dilution in Western blotting; Anti-GFP antibody (Santa Cruz;sc-9996) was used at 1:2000 dilution in Western blotting; Anti-Flag (Sigma; F3165) antibody was used at 1:000 dilution in Western blotting; Anti-Hsp70 (Abclonal; A0284) antibody was used at 1:000 dilution in Western blotting; Goat-anti-mouse HRP IgG (Santa Cruz; sc-2004) was used at 1:2000 dilution in Western blotting; Goat-anti-rat HRP IgG (Santa Cruz; sc-2005) was used at 1:2000 dilution in Western blotting; Goat-anti-mouse IRDye 800CW secondary antibody (licor; 926–32210) was used at 1:10,000 dilution. Goat-anti-rabbit IRDye 800CW secondary antibody (licor; 926–32211) was used at 1:10,000 dilution. Alexa Fluor 488 goat-anti-mouse IgG (Life technologies; 1298479) was used at 1:200 dilution in immunofluorescence.

4.5. Luciferase activity

Supernatants were taken from cell medium and mixed with equal volume of 2 × passive lysis buffer (Promega). Luciferase activity was measured with Renilla luciferase substrate (Promega) according to the manufacturer's protocol.

4.6. Transfection

For plasmid transfection, HEK293T cells were seeding onto poly-L-lysine (Sigma)-coated 6-well plates at a density of 4.5×10^5 cells/ml or Huh7 cells were seeding onto 6-well plates at a density of 2.5×10^5 cells/ml, and then transfected with plasmids using a TransIT-LT1 transfection kit (Mirus) according to the manufacturer's protocol. For RNA transfection, Huh7.5 cells were seeding onto 48-well plates at a density of 2.5×10^5 cells/ml and then transfected with 0.25μg *in-vitro*-transcribed RNA using a TransIT-mRNA transfection kit (Mirus) according to the manufacturer's protocol.

4.7. Western blotting

After washing with PBS, cells were lysed with 2 × SDS loading buffer (100 mM Tris-Cl [pH 6.8], 4% SDS, 0.2% bromophenol blue, 20% glycerol, 10% 2-mercaptoethanol) and then boiled for 5 min. Proteins were separated by SDS-PAGE and transferred to a nitrocellulose membrane. The membranes were incubated with blocking buffer (PBS, 5% milk, 0.05% Tween) for 1 h and then with primary antibody diluted in the blocking buffer. After three washes with PBST (PBS, 0.05% Tween), the membranes were incubated with secondary antibody. After three washes with PBST, the membrane was visualized by Western Lightning Plus-ECL substrate (PerkinElmer, NEL10500) or by *Odyssey CLx* Imaging System. The protein bands were quantified by densitometry with ImageJ if necessary.

4.8. Immunofluorescence and microscopy

Cells were fixed with 4% paraformaldehyde in PBS for 10 min at room temperature. After three washes with PBS, the cells were immunostained with antibodies as described previously (Yi et al., 2012). Or the coverslips were directly mounted with Mowiol. The coverslips were observed with a Leica TCS SP8 confocal laser microscopy with a 63 × numerical aperture 1.3 oil immersion objective. Images were captured with the LAS software and processed with ImageJ.

4.9. Cell fractionation

Huh7 cells were seeded into six-well plates and, after transfection, scraped into 400 µl hypotonic buffer (5 mM Tris-Cl [pH 7.5], 15 mM KCl, 2.5 mM MgCl2). After 15 min swelling on ice, the cells were passed 20 times through a 27-gauge needle and then centrifuged (900 × *g* for 5 min) to remove nuclei. One-tenth volume of 5 M NaCl was added or not to the postnuclear supernatants, and after incubation on ice for 20 min, the membranes were collected by centrifugation at 15,000 × *g* for 20 min. Pellets (membrane fraction, P) were resuspended in 30µl sodium dodecyl sulfate (SDS) loading buffer. Proteins in the supernatant (cytosol fraction, S) were concentrated by adding 4 vol of methanol, centrifuged (10 min, 12,000 × *g*), and resuspended in 30µl SDS loading buffer.

4.10. Proteinase K digestion

Cells in 6-well plates were permeabilized with 1ml 50 µg/ml digitonin in buffer C (20 mM HEPES-KOH [pH 7.7], 110 mM potassium acetate, 2 mM magnesium acetate, 1 mM EDTA) at room temperature for 5min, then scraped into 400 µl buffer C, and incubated with or without 10 µg/ml proteinase K for 5min at 37°C. Proteins were precipitated by adding equal volume of 40% TCA (trichloroacetic acid). After centrifugation at 12000 × *g* for 10min, the precipitates were washed by 500 µl acetone, and then dissolved in 30 µl 2D buffer (7M Urea, 2M thiourea). The samples were mixed with equal volumes 2 × SDS loading buffer and boiled for 5 min and then analyzed by Western blotting.

4.11. Immunoprecipitation

Cells in 6-well plates were lysed with 150 µl lysis buffer (50 mM TrisCl [pH 7.5], 1 mM EDTA, 15 mM MgCl2, 10 mM KCl, 1% Triton X-100, proteinase inhibitor [Roche]). Then cell lysates were passed through a 27-gauge needle 20 times and centrifuged at 12000 × *g* for 10min. 15 µl of the supernatant was taken and mixed with equal volume of 2 × SDS loading buffer as input (10%). The rest of the clarified cell lysates were incubated with 10 µl anti-HA magnetic beads (Pierce, SB246262) overnight with rotation at 4°C. After four washes with wash buffer (50 mM TrisCl [pH 7.5], 1 mM EDTA, 15 mM MgCl2, 10 mM KCl, 1% Triton X-100), the beads were lysed with 2 × SDS loading buffer. The samples were boiled for 10 min then analyzed by Western blotting.

Funding information

This work was in part supported by National Natural Science Foundation of China (81772181 to Yi, Z) and the Ministry of Science and Technology of the People's Republic of China (MOST) (2015CB554301 to Yi, Z). The funders had no role in study design, data collection and analysis, decision to publish, or preparation of the manuscript.

Conflicts of interest

The authors declare that they have no conflicts of interest with the contents of this article.

Yang Zhang, No conflict of interest.
Xiaomin Zhao, No conflict of interest.
Jingyi Zou, No conflict of interest.
Zhenghong Yuan, No conflict of interest.
Zhigang Yi, No conflict of interest.

Acknowledgements

We are grateful to Charles Rice (Rockefeller University) for providing the HCV reagents; to Wuhui Song (Fudan university) for her excellent technical assistance.

Abbreviations

HCV	hepatitis C virus
HCC	hepatocellular carcinoma
NS5A	nonstructural protein 5A
ER	endoplasmic reticulum
DMV	double membrane vesicle
RC, AH	amphipathic helix; replication complexes
SDS-PAGE	SDS-polyacrylamide gel electrophoresis
PK	proteinase K
WT	wild type
IP	immunoprecipitation

References

Appel, N., Zayas, M., Miller, S., Krijnse-Locker, J., Schaller, T., Friebe, P., Kallis, S., Engel, U., Bartenschlager, R., 2008. Essential role of domain III of nonstructural protein 5A for hepatitis C virus infectious particle assembly. PLoS Pathog. 4, e1000035.
Bachmair, A., Finley, D., Varshavsky, A., 1986. In vivo half-life of a protein is a function of its amino-terminal residue. Science 234, 179–186.
Biswas, A., Treadaway, J., Tellinghuisen, T.L., 2016. Interaction between nonstructural proteins NS4B and NS5A is essential for proper NS5A localization and hepatitis C virus RNA replication. J. Virol. 90, 7205–7218.
Brass, V., Bieck, E., Montserret, R., Wolk, B., Hellings, J.A., Blum, H.E., Penin, F., Moradpour, D., 2002. An amino-terminal amphipathic alpha-helix mediates membrane association of the hepatitis C virus nonstructural protein 5A. J. Biol. Chem. 277, 8130–8139.
Brass, V., Pal, Z., Sapay, N., Deleage, G., Blum, H.E., Penin, F., Moradpour, D., 2007. Conserved determinants for membrane association of nonstructural protein 5A from hepatitis C virus and related viruses. J. Virol. 81, 2745–2757.
Chong, W.M., Hsu, S.C., Kao, W.T., Lo, C.W., Lee, K.Y., Shao, J.S., Chen, Y.H., Chang, J., Chen, S.S., Yu, M.J., 2016. Phosphoproteomics identified an NS5A phosphorylation site involved in hepatitis C virus replication. J. Biol. Chem. 291, 3918–3931.
den Boon, J.A., Ahlquist, P., 2010. Organelle-like membrane compartmentalization of positive-strand RNA virus replication factories. Annu. Rev. Microbiol. 64, 241–256.
Dujardin, M., Madan, V., Montserret, R., Ahuja, P., Huvent, I., Launay, H., Bartenschlager, R., Penin, F., Lippens, G., Hanoulle, X., 2015. A Proline-Tryptophan turn in the intrinsically disordered domain 2 of NS5A protein is essential for Hepatitis C virus RNA replication. Protein Sci. 24, 121–122.
Elazar, M., Cheong, K.H., Liu, P., Greenberg, H.B., Rice, C.M., Glenn, J.S., 2003. Amphipathic helix-dependent localization of NS5A mediates hepatitis C virus RNA replication. J. Virol. 77, 6055–6061.
Evans, M.J., Rice, C.M., Goff, S.P., 2004. Phosphorylation of hepatitis C virus nonstructural protein 5A modulates its protein interactions and viral RNA replication. Proc. Natl. Acad. Sci. U. S. A 101, 13038–13043.
Gimenez-Andres, M., Copic, A., Antonny, B., 2018. The many faces of amphipathic helices. Biomolecules 8.
Gosert, R., Jendrsczok, W., Berke, J.M., Brass, V., Blum, H.E., Moradpour, D., 2005. Characterization of nonstructural protein membrane anchor deletion mutants expressed in the context of the hepatitis C virus polyprotein. J. Virol. 79, 7911–7917.
Gouttenoire, J., Castet, V., Montserret, R., Arora, N., Raussens, V., Ruysschaert, J.M., Diesis, E., Blum, H.E., Penin, F., Moradpour, D., 2009. Identification of a novel determinant for membrane association in hepatitis C virus nonstructural protein 4B. J. Virol. 83, 6257–6268.
Gouttenoire, J., Montserret, R., Paul, D., Castillo, R., Meister, S., Bartenschlager, R., Penin, F., Moradpour, D., 2014. Aminoterminal amphipathic alpha-helix AH1 of hepatitis C virus nonstructural protein 4B possesses a dual role in RNA replication and virus production. PLoS Pathog. 10, e1004501.
Gouttenoire, J., Roingeard, P., Penin, F., Moradpour, D., 2010. Amphipathic alpha-helix AH2 is a major determinant for the oligomerization of hepatitis C virus nonstructural protein 4B. J. Virol. 84, 12529–12537.
Gu, M., Rice, C.M., 2013. Structures of hepatitis C virus nonstructural proteins required for replicase assembly and function. Curr. Opin. Virol. 3, 129–136.
Kato, T., Date, T., Miyamoto, M., Zhao, Z., Mizokami, M., Wakita, T., 2005. Nonhepatic cell lines HeLa and 293 support efficient replication of the hepatitis C virus genotype 2a subgenomic replicon. J. Virol. 79, 592–596.
Koch, J.O., Bartenschlager, R., 1999. Modulation of hepatitis C virus NS5A hyperphosphorylation by nonstructural proteins NS3, NS4A, and NS4B. J. Virol. 73, 7138–7146.
Lam, A.M., Edwards, T.E., Mosley, R.T., Murakami, E., Bansal, S., Lugo, C., Bao, H., Otto, M.J., Sofia, M.J., Furman, P.A., 2014. Molecular and structural basis for the roles of hepatitis C virus polymerase NS5B amino acids 15, 223, and 321 in viral replication and drug resistance. Antimicrob. Agents Chemother. 58, 6861–6869.
Lin, C., Pragai, B.M., Grakoui, A., Xu, J., Rice, C.M., 1994. Hepatitis C virus NS3 serine proteinase: trans-cleavage requirements and processing kinetics. J. Virol. 68, 8147–8157.
Liu, L., Westler, W.M., den Boon, J.A., Wang, X., Diaz, A., Steinberg, H.A., Ahlquist, P., 2009. An amphipathic alpha-helix controls multiple roles of brome mosaic virus

protein 1a in RNA replication complex assembly and function. PLoS Pathog. 5, e1000351.
Love, R.A., Brodsky, O., Hickey, M.J., Wells, P.A., Cronin, C.N., 2009. Crystal structure of a novel dimeric form of NS5A domain I protein from hepatitis C virus. J. Virol. 83, 4395–4403.
Lundin, M., Monne, M., Widell, A., Von Heijne, G., Persson, M.A., 2003. Topology of the membrane-associated hepatitis C virus protein NS4B. J. Virol. 77, 5428–5438.
Manns, M.P., Buti, M., Gane, E., Pawlotsky, J.M., Razavi, H., Terrault, N., Younossi, Z., 2017. Hepatitis C virus infection. Nat. Rev. Dis. Prim. 3, 17006.
Martyna, A., Bahsoun, B., Badham, M.D., Srinivasan, S., Howard, M.J., Rossman, J.S., 2017. Membrane remodeling by the M2 amphipathic helix drives influenza virus membrane scission. Sci. Rep. 7, 44695.
Moradpour, D., Penin, F., Rice, C.M., 2007. Replication of hepatitis C virus. Nat. Rev. Microbiol. 5, 453–463.
Paul, D., Hoppe, S., Saher, G., Krijnse-Locker, J., Bartenschlager, R., 2013. Morphological and biochemical characterization of the membranous hepatitis C virus replication compartment. J. Virol. 87, 10612–10627.
Penin, F., Brass, V., Appel, N., Ramboarina, S., Montserret, R., Ficheux, D., Blum, H.E., Bartenschlager, R., Moradpour, D., 2004. Structure and function of the membrane anchor domain of hepatitis C virus nonstructural protein 5A. J. Biol. Chem. 279, 40835–40843.
Romero-Brey, I., Berger, C., Kallis, S., Kolovou, A., Paul, D., Lohmann, V., Bartenschlager, R., 2015. NS5A domain 1 and polyprotein cleavage kinetics are critical for induction of double-membrane vesicles associated with hepatitis C virus replication. mBio 6, e00759.
Romero-Brey, I., Merz, A., Chiramel, A., Lee, J.Y., Chlanda, P., Haselman, U., Santarella-Mellwig, R., Habermann, A., Hoppe, S., Kallis, S., Walther, P., Antony, C., Krijnse-Locker, J., Bartenschlager, R., 2012. Three-dimensional architecture and biogenesis of membrane structures associated with hepatitis C virus replication. PLoS Pathog. 8, e1003056.
Ross-Thriepland, D., Amako, Y., Harris, M., 2013a. The C terminus of NS5A domain II is a key determinant of hepatitis C virus genome replication, but is not required for virion assembly and release. J. Gen. Virol 94, 1009–1018.
Ross-Thriepland, D., Amako, Y., Harris, M., 2013b. The C terminus of NS5A domain II is a key determinant of hepatitis C virus genome replication, but is not required for virion assembly and release. J. Gen. Virol. 94, 1009–1018.
Shanmugam, S., Nichols, A.K., Saravanabalaji, D., Welsch, C., Yi, M., 2018. HCV NS5A dimer interface residues regulate HCV replication by controlling its self-interaction, hyperphosphorylation, subcellular localization and interaction with cyclophilin A. PLoS Pathog. 14, e1007177.
Tellinghuisen, T.L., Marcotrigiano, J., Rice, C.M., 2005. Structure of the zinc-binding domain of an essential component of the hepatitis C virus replicase. Nature 435, 374–379.
Verdegem, D., Badillo, A., Wieruszeski, J.M., Landrieu, I., Leroy, A., Bartenschlager, R., Penin, F., Lippens, G., Hanoulle, X., 2011. Domain 3 of NS5A protein from the hepatitis C virus has intrinsic alpha-helical propensity and is a substrate of cyclophilin A. J. Biol. Chem. 286, 20441–20454.
Xu, X., Song, H., Qi, J., Liu, Y., Wang, H., Su, C., Shi, Y., Gao, G.F., 2016. Contribution of intertwined loop to membrane association revealed by Zika virus full-length NS1 structure. EMBO J. 35, 2170–2178.
Yi, Z., Fang, C., Zou, J., Xu, J., Song, W., Du, X., Pan, T., Lu, H., Yuan, Z., 2016. Affinity purification of the hepatitis C virus replicase identifies valosin-containing protein, a member of the ATPases associated with diverse cellular activities family, as an active virus replication modulator. J. Virol. 90, 9953–9966.
Yi, Z., Pan, T., Wu, X., Song, W., Wang, S., Xu, Y., Rice, C.M., Macdonald, M.R., Yuan, Z., 2011. Hepatitis C virus co-opts Ras-GTPase-activating protein-binding protein 1 for its genome replication. J. Virol. 85, 6996–7004.
Yi, Z., Yuan, Z., Rice, C.M., MacDonald, M.R., 2012. Flavivirus replication complex assembly revealed by DNAJC14 functional mapping. J. Virol. 86, 11815–11832.
Zhang, Y., Zou, J., Zhao, X., Yuan, Z., Yi, Z., 2019. Hepatitis C virus NS5A inhibitor daclatasvir allosterically impairs NS4B-involved protein-protein interactions within the viral replicase and disrupts the replicase quaternary structure in a replicase assembly surrogate system. J. Gen. Virol 100, 69–83.